CALCIUM SPECIATION AND ORGANIC CARBON RESPONSE TO ACIDIFICATION IN KARST CULTIVATED SOILS OF HUNAN

DUAN, C. L.[1] – YUAN, H.[1,2*] – XIN, Y. X.[1] – DING, H. S.[1] – JI, X. T.[1] – LIU, P.[1] – HE, Y. H.[1] – ZENG, G.[1] – ZHANG, L. J.[1] – JIANG, J.[1] – XIE, H. X.[1] – SHENG, H.[1]

[1]*College of Resources, Hunan Agricultural University, Changsha, Hunan 410128, China*

[2]*Karst Dynamics Laboratory, MNR, and GZAR (Institute of Karst Geology, CAGS) Guilin Guangxi 541004, China*

[*]*Corresponding author*
e-mail: brandyuan@163.com; phone: +86-151-1628-7243

(Received 25th Aug 2025; accepted 3rd Dec 2025)

Abstract. To clarify the mechanisms of acid suppression and enhancement of soil quality, this study investigated the interaction between calcium and carbon during soil acidification in karst arable land in Hunan, China. Soil samples were categorized into four acidification grades: strong (pH ≤ 4.5), weak (4.5 < pH ≤ 6.5), neutral (6.5 < pH ≤ 7.5), and alkaline (pH > 7.5). The relationship between soil calcium speciation and acidification was examined. A sequential variation in calcium content was observed across different speciation in the following order: exchangeable calcium, acid-soluble calcium, water-soluble calcium, residual calcium, and organically bound calcium. Active calcium migration in the study area reflected its bioavailability. Compared with alkaline conditions, soil calcium, carbon content, and carbon storage decreased with increasing soil acidification ($p < 0.05$). The average soil organic carbon (SOC) content declined from 44.4% to 34.3%, and the carbon stock decreased from 41.4% to 28.4%. A significant correlation was found between the total soil calcium and organic carbon content ($p < 0.05$). Under strong acidification, the calcium and carbon contents, as well as the carbon stocks, reached their lowest levels, resulting in a 215-fold decrease in calcium effectiveness. The primary factors contributing to soil acidification in this area were the soil calcium levels and morphology. Enhancing SOC content and improving the activity of Ca^{2+} in karst soils serve as mechanisms for acid suppression.
Keywords: *karst areas, cropland, soil acidification, calcium speciation, soil organic carbon*

Introduction

Agricultural land plays a pivotal role in sustaining human civilization (Fan et al., 2020), serving multiple essential functions, including agricultural production, the provision of spatial resources, and environmental conservation (Qiu et al., 2023). This resource is fundamentally connected to national food security and social stability, while also promoting sustainable economic development (Zhang and Qie, 2024). Acidic soil conditions in agricultural areas represent a significant manifestation of global soil degradation and are a pressing ecological concern, particularly in southwestern China. Characterized by declining soil pH levels and increasing exchangeable acidity (Xu et al., 2018), this phenomenon poses a substantial risk to agricultural yield security and the sustainability of agricultural practices (Luo et al., 2018).

Karst habitats, primarily found in tropical and subtropical regions, are characterized by the transformation of carbonate bedrock into limestone soils through dissolution and weathering processes. This unique karst landscape promotes complex soil-formation processes. Although the precise mechanisms of soil formation remain unclear, karst dynamics have significantly influenced the development of limestone soils. These soils

http://www.aloki.hu ● ISSN 1589 1623 (Print) ● ISSN1785 0037 (Online)
DOI: http://dx.doi.org/10.15666/aeer/2401_885903

exhibit unique geochemical signatures, marked by elevated calcium levels and alkaline properties, as extensively documented in geological literature (Cao et al., 2004).

Karst regions in China cover an area of 3.443 million square kilometers, accounting for more than one-third of the country's total land area. The southwestern region encompasses approximately 411,000 square kilometers and is characterized by distinctive karst formations. This region is recognized as one of the world's three major centers for karst distribution and is the largest continuous karst zone (Wang et al., 2018; Ma et al., 2020). Karst landscapes are extremely fragile and highly sensitive to environmental change. It has a limited capacity to support natural ecosystems, lacks resilience to disasters, and suffers significant damage from human activities. Moreover, it is important to note that this area is among the most severely affected locations in China in terms of soil acidification, as demonstrated in previous studies (Li et al., 2005; Duan et al., 2016; Tao et al., 2019). In karst hills and mountainous regions, plant growth is hindered by complex and variable natural conditions, diverse soil compositions, infertile soils, and a scattered distribution (Yi et al., 2025). The availability of land resources is highly uneven, making arable land more valuable than that found in plains and exacerbating the inherent tension between human needs and land availability.

The material cycle in karst systems is predominantly characterized by the C-H_2O-Ca cycle, which results in the formation of a geochemical environment rich in calcium and alkaline in nature. Calcium is the primary biological component of karst habitats. The enrichment and migration of substances are closely connected to the soil quality of karst arable land, which significantly affects soil acidity, alkalinity, and organic carbon accumulation (Nava et al., 2020; Yang et al., 2021). Maintaining soil quality in karst arable soils depends heavily on the acid-base equilibrium, which is regulated by the presence of calcium and organic carbon within these ecosystems. Numerous studies have investigated the importance of calcium in karst ecosystems. The primary focus of these studies was to assess the effects of calcium on heavy metal adsorption, microbial communities, plant life, and other species (Wei et al., 2004; Hen et al., 2014; Wei et al., 2017; Liu et al., 2021). In addition, these investigations explored the influence of environmental conditions on the calcium distribution (Li et al., 2012, 2016; Yang et al., 2015; Huang et al., 2024). Studies on karst arable land have primarily focused on evaluating soil quality, particularly in terms of soil nutrients, microorganisms, bacterial activity (Gao et al., 2023), resistance to soil erosion (Xiao et al., 2019), overall soil quality (Zhang et al., 2021), and ecological safety (Jiang et al., 2022; Wu et al., 2023). However, there has been limited research on the mechanisms and effects of calcium and carbon in mitigating acidification in karst farmland soils.

Soil acidification in Hunan Province has intensified owing to irrational agricultural practices, excessive cultivation, and heavy use of agrochemicals. During the second soil census, the average pH value of arable soils decreased from 6.5 to the current 6.0. Although limestone weathering materials originate from alkaline parent rocks, and the karst soils formed from them exhibit neutral to alkaline characteristics, the widespread acidification of soils in Hunan significantly undermines the capacity of the province to produce grains (Wen et al., 2013). The acidity levels in karst soils are increasing. Both the natural environment and human agricultural activities exacerbate soil acidity in karst arable lands. Further research is necessary to investigate the imbalance in the calcium components in karst soils (Zhang et al., 2022; Lin, 2022).

This study determined the distribution locations, ranges, and areas of karst areas in Hunan province using geological, topographic, land-use status, karst geomorphology

http://www.aloki.hu ● ISSN 1589 1623 (Print) ● ISSN1785 0037 (Online)
DOI: http://dx.doi.org/10.15666/aeer/2401_885903

zoning, and matrix zoning maps. Key data regarding the distribution locations, ranges, and areas of karst regions in Hunan were collected. Soil profile sampling points were established in primary karst distribution areas based on field surveys. This study investigated the response and interaction between calcium and carbon in karst soils under varying acidification conditions using soil pH acidification grading. This study aims to provide a scientific foundation for the conservation of karst arable land quality and food security in Hunan Province.

Materials and methods

Study area and soil sampling

The specimens were collected from the characteristic spatial distribution region of the karst parent materials in Hunan Province (*Figure 1*). Situated in the northern subtropics, Hunan Province experiences a humid subtropical monsoon climate, characterized by an average annual temperature ranging from 16°C to 18°C and an average annual precipitation of 1200–1800 mm. This region is renowned for its humid climate, four distinct seasons, and intense rainfall.

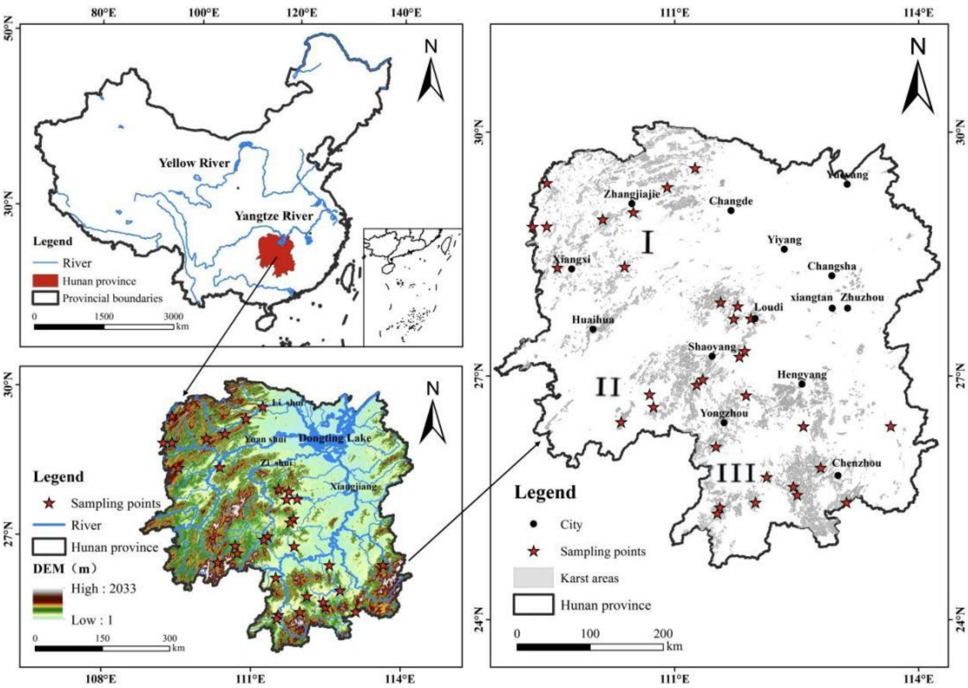

Figure 1. Distribution of soil sampling points in karst cultivated land in Hunan Province

The total area of the karst region in Hunan Province is 5.4964 million hectares, accounting for 25.95% of the province’s total land area (Zhou et al., 2020). These karst regions are primarily concentrated in Zhangjiajie, Shaoyang, Chenzhou, and other areas in northwestern, central-western, and southern Hunan Provinces. The three major areas represent distinct karst geomorphological types: hill-peak-to-solution basin and solution depression in canyon-mountain plateau areas, hill-peak-to-solution depression and solution basin in low mountain and hilly areas, and hill-peak-to-peak forest to solution basin and solution depression in hilly plain areas.

http://www.aloki.hu ● ISSN 1589 1623 (Print) ● ISSN1785 0037 (Online)
DOI: http://dx.doi.org/10.15666/aeer/2401_885903

This study involved the selection of karst soils with varying pH levels from representative karst regions in the Hunan Province. These soils were categorized into four groups for spot sampling: extremely acidified (pH ≤ 4.5), weakly to moderately acidified (4.5 < pH ≤ 6.5), neutral (6.5 < pH ≤ 7.5), and alkaline (pH > 7.5). *Fig. 1* and *Table A1* show the distributions of the selected soil sampling sites. Appropriate sampling locations in representative karst regions were selected based on the criteria established for the soil field investigation. The soil profiles were excavated to a depth of 150 cm below the surface or until the paralithic contact surface or lower boundary of the diagnostic subsurface horizon was reached. The morphological features of each horizon were meticulously documented in accordance with the field soil description and sampling criteria outlined in the Chinese soil systematics. Based on the physical characteristics of the profile, the soil horizons were categorized, and soil samples weighing 1.5 to 2.0 kg were collected for laboratory analysis from the bottom to the top of each horizon. Soil bulk density, moisture content, and porosity were analyzed by collecting undisturbed soil samples from top to bottom using the ring-knife technique. The soil horizon samples were naturally air-dried, pulverized, and sieved using 10-mesh, 60-mesh, and 100-mesh sieves. They were then blended, labeled, and stored for quantitative analysis of fundamental physical and chemical characteristics as well as various forms of calcium content.

Analyses of soil physiochemical properties

The fundamental physicochemical properties of the soil were assessed using conventional analytical methods as previously described (Dong et al., 2019). The soil pH was measured using the potassium chloride extraction potentiometric method. The soil organic matter content was quantified using the potassium dichromate–sulfuric acid digestion method. The soil moisture content was determined using a drying method. Soil bulk density was assessed using the core sampling technique. The mechanical composition was analyzed using the pipette method. Soil cation exchange capacity (CEC) was measured using the 1 mol/L ammonium acetate extraction method. The speciation of calcium in the soil was determined using the modified BCR sequential extraction method (Yu et al., 2007), which categorizes soil calcium into five species: water-soluble calcium (WSC), exchangeable calcium (EC), acid-soluble calcium (ASC), organically bound calcium (OBC), and residual calcium (RC). The specific operational steps are listed in *Table A2*.

Data analyses

The soil organic carbon (SOC) density of soil layer i was calculated as

$$SOCD_i = SOCC_i \cdot BD_i \cdot H_i \,/\, 100 \qquad \text{(Eq.1)}$$

where SOCDi is SOC density (kg m^{-2}) in layer i, SOCCi is organic carbon content (g kg^{-1}) in layer i, BDi is soil bulk density (g cm^{-3}) in layer i, and Hi is the thickness of soil in layer i (cm).

SOC storage (SOCS) in the profile was calculated as:

$$SOCS(kgm^{-2}) = BD_i \cdot H_i \,/\, 100 \qquad \text{(Eq.2)}$$

where n is the number of layers in the soil profile.

http://www.aloki.hu ● ISSN 1589 1623 (Print) ● ISSN1785 0037 (Online)
DOI: http://dx.doi.org/10.15666/aeer/2401_885903

All data are presented as mean ± standard deviation computed using Origin 2018 and Microsoft Excel 2010 software. One-way analysis of variance and the least significant difference test ($p < 0.05$) were conducted using SPSS V21 to assess the variations among the treatments. Path analysis for structural equation modeling was performed using R version 4.4.0 (Dion et al., 2021), whereas redundancy analysis (RDA) was performed using Canoco 5 software.

Results

Changes in SOC

Characteristics of soil tillage layer

As shown in *Figure 2* and *Table 1*, the content and stock of soil organic carbon in the plough layer were lowest under weakly to moderately acidic conditions. Total nitrogen (TN), total potassium (TK), cation exchange capacity (CEC), and the contents of sand and silt exhibited trends consistent with those of soil organic carbon, declining in neutral to weakly acidic regions, with TN and TK showing significant changes ($p < 0.05$). The reductions in SOC content and storage were 31.6% and 37.84%, respectively. In addition, the TN, TK, and CEC decreased by 30.8%, 14.2%, and 22.2%, respectively, whereas the sand and silt fractions in the soil's mechanical composition decreased by 21.5% and 0.53%, respectively. Consequently, the nitrogen content and soil fertility retention capacity of the cultivated layer in the karst farmland of Hunan Province significantly diminished owing to acidification.

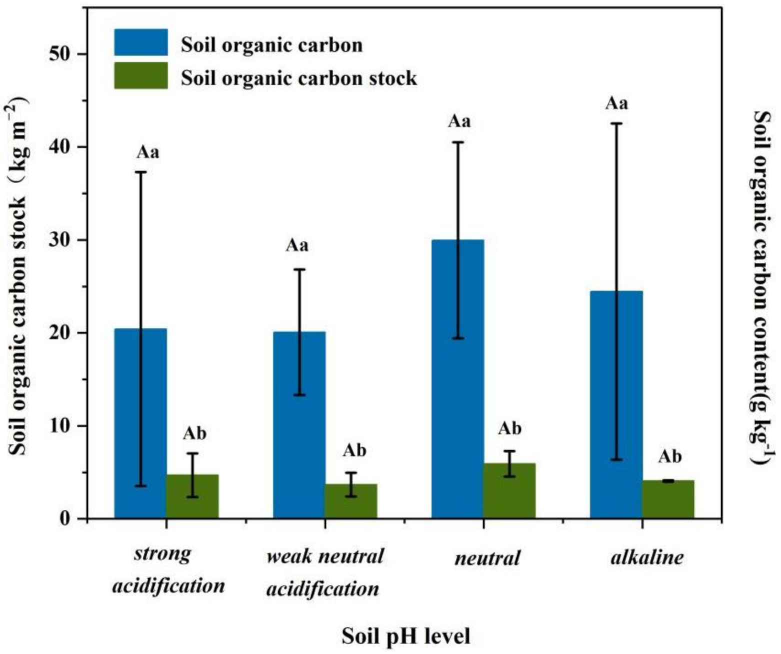

Figure 2. *Relationships between organic carbon content, soil tillage storage, and pH under different acidification conditions. NO: Distinct capital letters indicate significant (p < 0.05) differences in organic carbon and stocks across various acid-base categories, whereas distinct lowercase letters denote differences in organic carbon and stocks within the same acid-base classifications (p < 0.05)*

http://www.aloki.hu ● ISSN 1589 1623 (Print) ● ISSN1785 0037 (Online)
DOI: http://dx.doi.org/10.15666/aeer/2401_885903

Table 1. *Analysis of basic physicochemical properties of tillage soil under different soil acidity and alkalinity classifications*

	Strong acidification (n=8)	**Weak neutral acidification (n=5)**	**Neutral (n=5)**	**Alkaline (n=2)**
Soil pH	3.92 ± 0.33d	5.20 ± 0.47c	6.96 ± 0.18b	7.56 ± 0.08a
SOC (g kg^{-1})	20.41 ± 16.89a	20.07±6.73a	29.35±11.668a	24.45±18.08a
CEC (cmol (+) kg^{-1})	19.32 ± 6.62a	16.38 ± 5.6a	21.04 ± 3.36a	15.15 ± 1.34a
Sand grains (%)	68 ± 53.32a	73 ± 48.69a	93 ± 63.49a	361 ± 274.35a
Silt grains (%)	357 ± 154.02a	563.2 ± 58.98a	566.2 ± 110.45a	402 ± 270.11a
Clay particles (%)	574.75 ± 188a	363.8 ± 25.87ab	340.2 ± 127.94b	237 ± 4.24b
TN (g kg^{-1})	1.46 ± 0.93a	1.57 ± 0.37ab	2.27 ± 0.75b	2.29 ± 1.67b
TP (g kg^{-1})	0.44 ± 0.16b	1.03 ± 0.42a	0.78 ± 0.19ab	0.49 ± 0.26b
TK (g kg^{-1})	14.55 ± 3.77a	12.45 ± 3.75ab	14.51 ± 3.2a	7.72 ± 2.19b

NO: Different letters in the same column indicate significant differences (p < 0.05) in various physicochemical properties between acidification conditions

Soil profiles characteristics

Table 2 and *Figure 3* illustrate that the TN concentration in the soil, along with the trends in sand and silt particle composition, reflected a significant declining trend in SOC ($p < 0.05$). The mean organic carbon concentration throughout the entire profile of the karst agricultural soil in Hunan was 13.08 g kg^{-1}. Throughout the soil profile, SOC content and stock exhibited their minimum values under strongly acidic conditions. Comparing with medium alkaline conditions, the average SOC content and storage decreased by 44.4% to 34.3% and 41.4% to 28.4%, respectively. The observed decline in SOC content and storage within the profile of karst-cultivated soils in Hunan indicates that strong acidification has a more pronounced effect than weak neutral acidification.

Table 2. *Analysis of basic physicochemical properties of profiled soils under different acidification conditions*

Soil pH level	**Strong acidification (n=33)**	**Weak neutral acidification (n=25)**	**Neutral (n=24)**	**Alkaline (n=9)**
Soil pH	3.94 ± 0.24d	5.57 ± 0.45c	6.92 ± 0.26b	7.77 ± 0.15a
SOC (g kg^{-1})	9.30 ± 10.85a	12.12 ± 6.91a	16.74 ± 10.01.a	14.16 ± 10.19a
CEC (cmol(+) kg^{-1})	19.35 ± 6.83a	14.13 ± 3.69b	18.94 ± 3.79a	11.75 ± 5.69b
Sand grains (%)	73.97 ± 63.13b	117.44 ± 67.46ab	95.47 ± 68.93b	157.28 ± 27.78a
Silt grains (%)	300.94 ± 140.42b	570.28 ± 100.09a	542.12 ± 126.43a	620.86 ± 38.55a
Clay particles (%)	625.06 ± 176.98a	312.20 ± 73.28bc	362.41±129.72b	221.71 ± 25.38c
TN (g kg^{-1})	0.93 ± 0.57b	0.96 ± 0.42b	1.41 ± 0.67a	1.42 ± 0.87a
TP (g kg^{-1})	0.41 ± 0.13b	0..80 ± 0.46a	0.55 ± 0.19ab	0.38 ± 0.11b
TK (g kg^{-1})	16.46 ± 5.83a	13.30 ± 4.55ab	15.65 ± 3.92b	10.94 ± 2.52b

NO: Different letters in the same column indicate significant differences (p < 0.05) in various physicochemical properties between acidification conditions

http://www.aloki.hu ● ISSN 1589 1623 (Print) ● ISSN1785 0037 (Online)
DOI: http://dx.doi.org/10.15666/aeer/2401_885903

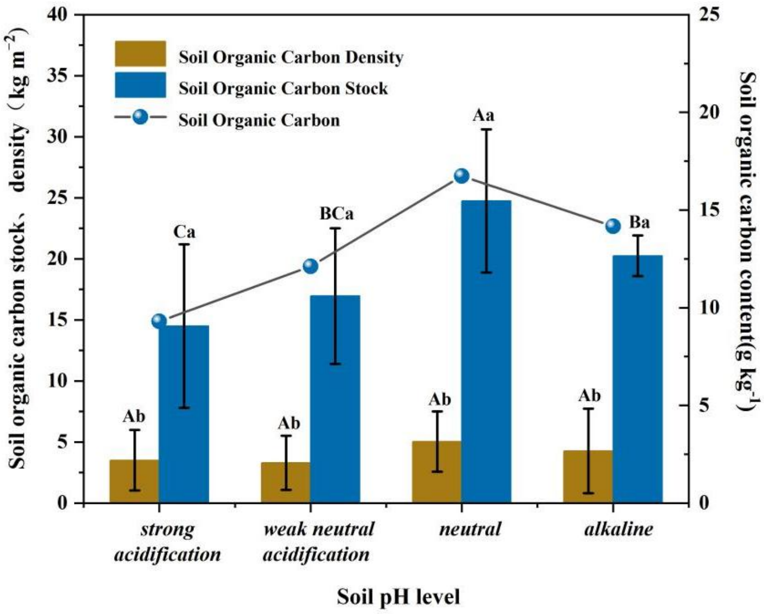

Figure 3. *Relationships between SOC content and storage, density, and pH in profiles under different acidification conditions. NO: Distinct uppercase letters denote significant differences ($p < 0.05$) in organic carbon density and stocks across varying acidity and alkalinity classes, whereas distinct lowercase letters indicate significant differences ($p < 0.05$) in organic carbon density and stocks within the same acidity and alkalinity class. Distinct uppercase letters denote substantial differences ($p < 0.05$) in organic carbon density and stocks across various acid-base classifications, whereas distinct lowercase letters indicate variances ($p < 0.05$) in organic carbon density and stocks within the same acid-base classification*

Changes in calcium speciation

In the cultivated karst soils of Hunan, calcium predominantly existed in exchangeable forms, accounting for approximately 94% of the total calcium species. The average concentrations were 13.4 g kg^{-1} in whole profiles and 29.02 g kg^{-1} in tillage layers. OBC constituted the smallest fraction, at 0.14% and 0.05%, respectively. The hierarchy of calcium speciation was as follows: EC > ASC > WSC > RC > OBC. Neutral to alkaline conditions increased calcium concentrations, demonstrating a strong pH dependence for WSC (*$p < 0.05$*). Soil acidification progressively reduced the WSC, EC, and ASC content, with EC showing a significant correlation with pH (*$p < 0.05$*). The transition from alkaline to acidic conditions resulted in a 215-fold decrease in calcium availability in the profiles and a 314-fold decrease in the tillage layers (*Tables 3,4* and *Figures 4,5*).

Changes in calcium/carbon ratio

This study demonstrated a significant progressive decline in the ratios of WSC, EC, ASC, and total calcium to organic carbon with increasing acidification, reaching minimum reductions of 98.95, 99.29, 96.03, and 98.82%, respectively, under severe acidification. Conversely, the proportions of RC and OBC relative to organic carbon progressively increased. Acidification significantly affects the availability of calcium and carbon in the karst farmland soils of Hunan Province, and the synergistic interaction between available calcium and organic carbon provides a scientific basis for mitigating acidification in karst ecosystems (*Figure 6*).

http://www.aloki.hu ● ISSN 1589 1623 (Print) ● ISSN1785 0037 (Online)
DOI: http://dx.doi.org/10.15666/aeer/2401_885903

Table 3. *Speciation profiling of calcium forms in tillage horizon soils across acidification gradient*

Soil pH level	Water-Soluble Ca/(g·kg^{-1})	Exchangeable Ca/(g·kg^{-1})	Acid-Soluble Ca/(g·kg^{-1})	Bound Ca/(g·kg^{-1})	Residual Ca/(g·kg^{-1})
Strong acidification (n=8)	0.0611 ± 0.313b	0.26 ± 0.231b	0.059 ± 0.048b	0.0168 ± 0.014a	0.068 ± 0.859a
Weak neutral acidification (n=5)	0.102 ± 0.513b	0.502 ± 0.225b	0.126 ± 0.067b	0.0178 ± 0.015a	0.064 ± 0.077a
Neutral (n=5)	0.521 ± 0.433a	26.32 ± 28.71b	1.398 ± 0.998b	0.0164 ± 0.01a	0.0136 ± 0.008ab
Alkaline (n=2)	0.6433 ± 0.383a	89.036 ± 100.5a	4.17 ± 4.61a	0.016 ± 0.016a	0.077 ± 0.005b

NO: Different lowercase letters in the same column indicate statistically significant differences ($p < 0.05$) in calcium content across different acidification conditions

Table 4. *Speciation profiling of calcium in soil profiles across acidification gradients*

Soil pH level	Water soluble Ca/(g·kg^{-1})	Exchangeable Ca/(g·kg^{-1})	Acid soluble Ca/(g·kg^{-1})	Bound Ca/(g·kg^{-1})	Residual Ca/(g·kg^{-1})
Strong acidification (n=33)	0.034 ± 0.026c	0.178 ± 0.245c	0.045 ± 0.05b	0.020 ± 0.016a	0.055 ± 0.069a
Weak neutral acidification (n=25)	0.073 ± 0.038c	0.591 ± 0.234c	0.114 ± 0.05b	0.021 ± 0.015a	0.062 ± 0.063a
Neutral (n=24)	0.37 ± 0.33b	20.69 ± 26.73b	1.030 ± 1.02a	0.021 ± 0.013a	0.026 ± 0.017ab
Alkaline (n=9)	0.183 ± 0.262a	32.17 ± 13.1a	1.280 ± 0.41a	0.016 ± 0.009a	0.012 ± 0.006b

NO: Different lowercase letters in the same column indicate statistically significant differences ($p < 0.05$) in calcium content across different acidification conditions

http://www.aloki.hu ● ISSN 1589 1623 (Print) ● ISSN1785 0037 (Online)
DOI: http://dx.doi.org/10.15666/aeer/2401_885903

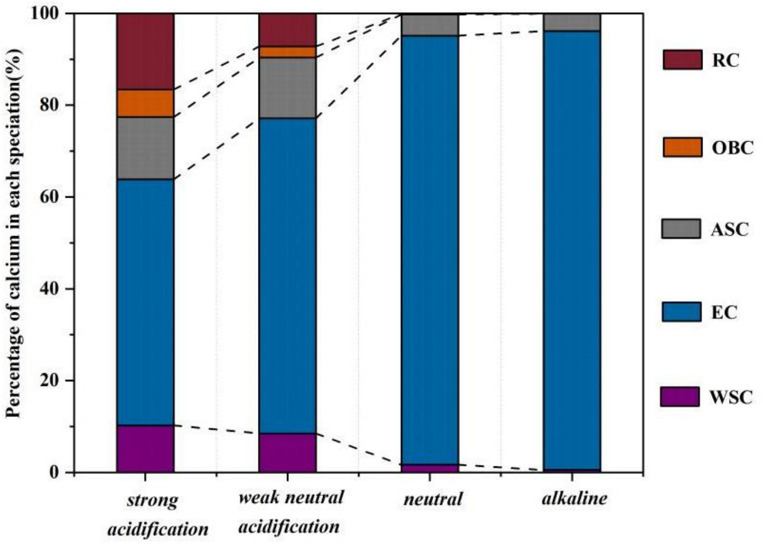

Figure 4. *Speciation composition of calcium in tillage horizon soils across acidification gradients*

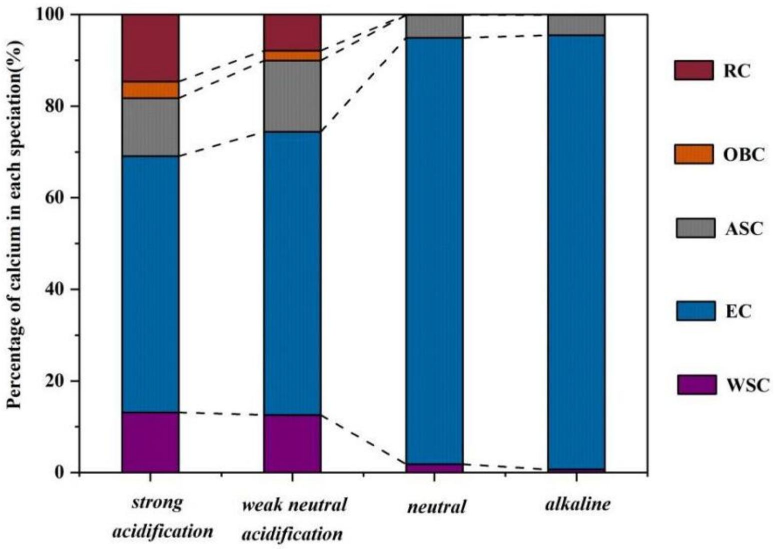

Figure 5. *Speciation composition of calcium in soil profiles across acidification gradients*

http://www.aloki.hu ● ISSN 1589 1623 (Print) ● ISSN1785 0037 (Online)
DOI: http://dx.doi.org/10.15666/aeer/2401_885903

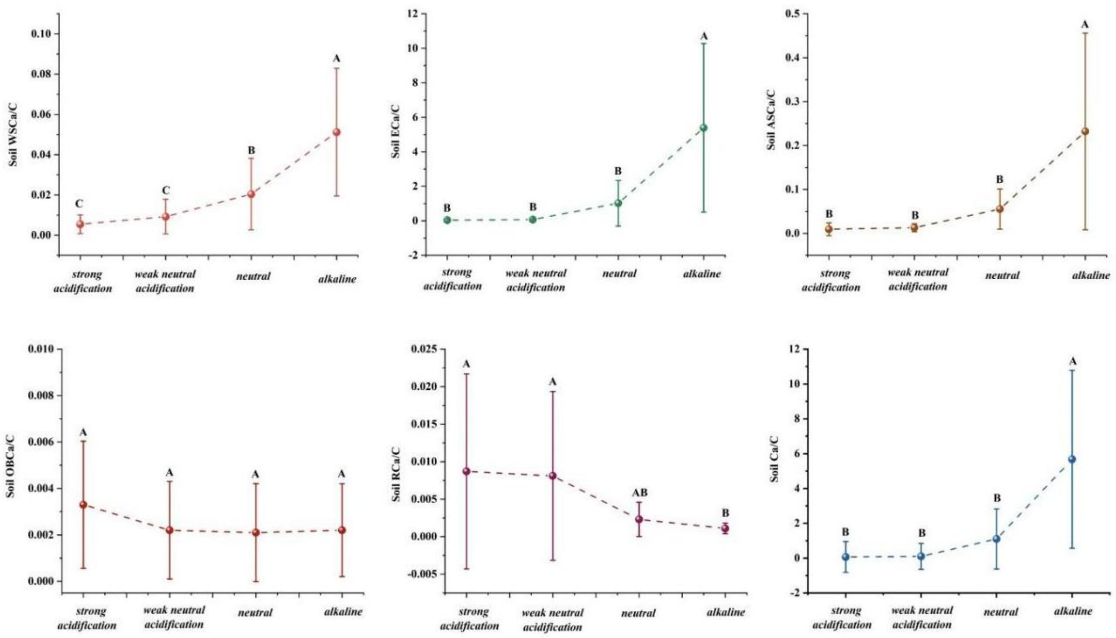

Figure 6. *Proportions of calcium species to organic carbon under diverse acidification conditions. NO: Different capital letters indicate significant differences ($p < 0.05$) in the calcium-to-carbon ratio across varying degrees of acidification*

Factor determinant evaluation and SEM projection analysis

We conducted RDA, a form of constrained principal component analysis, to identify the factors influencing calcium migration and transformation in the soils. This study examined SOC, essential physicochemical properties, and calcium speciation across systematically classified acidification gradients. This analytical method quantitatively assessed the correlations between environmental variables such as soil pH, organic carbon, CEC, particle size distribution, and multivariate calcium speciation data (Sanchez-Rodriguez et al., 2022; Gu et al., 2023). The RDA ordination plot (*Figure 7*) indicated that the acute angles between the arrows representing the environmental factors and ordination axes reflect stronger correlations. In addition, various forms of calcium demonstrated distinct responsiveness to specific soil parameters under different acidification conditions (Li et al., 2015).

http://www.aloki.hu ● ISSN 1589 1623 (Print) ● ISSN1785 0037 (Online)
DOI: http://dx.doi.org/10.15666/aeer/2401_885903

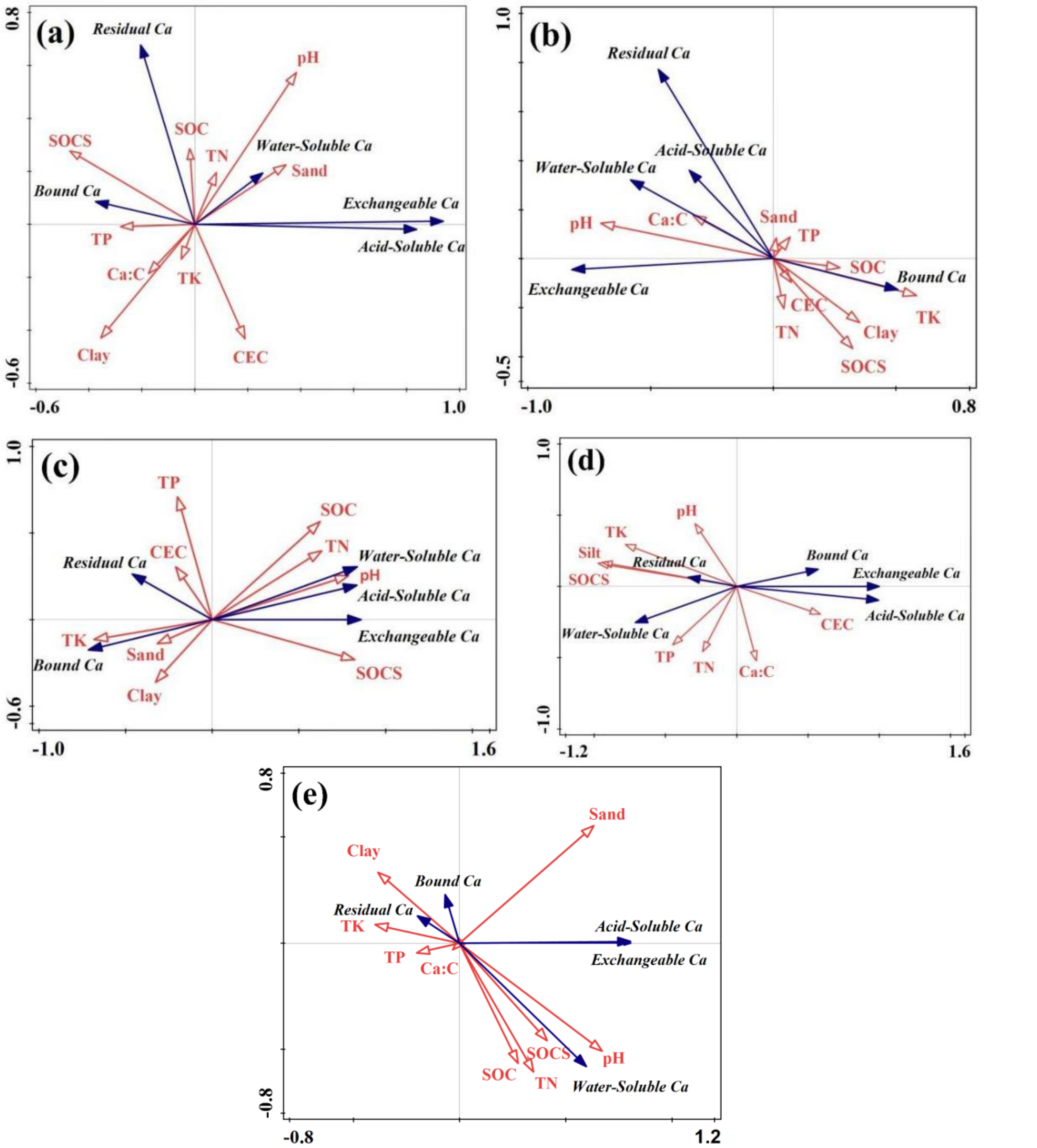

Figure 7. *RDA of calcium-carbon interplay in soils under different acidification scenarios. NO: strong acidification; (b) weak neutral acidification; (c) neutral; (d) alkaline; (e) no differentiation of acidification gradients*

Comparative studies revealed various correlation patterns under different pH conditions (*Figure 8*). In soils with weak to moderate acidification (pH 4.5–6.5), positive correlations were identified between soil pH and three critical parameters: SOC concentration, SOC storage capacity, and calcium-to-carbon (Ca/C) ratio. SOC measurements exhibited bidirectional links, demonstrating positive correlations with OBC and significant relationships with TN fertility ($p < 0.05$). Particle size analysis revealed significant discrepancies: strong positive relationships with silt fractions ($p < 0.01$), contrasted with considerable negative correlations with clay content ($p < 0.01$). Furthermore, the Ca/C ratio showed notable sensitivity to labile calcium forms, exhibiting the most significant correlation with EC and ASC fractions ($p < 0.01$).

http://www.aloki.hu ● ISSN 1589 1623 (Print) ● ISSN1785 0037 (Online)
DOI: http://dx.doi.org/10.15666/aeer/2401_885903

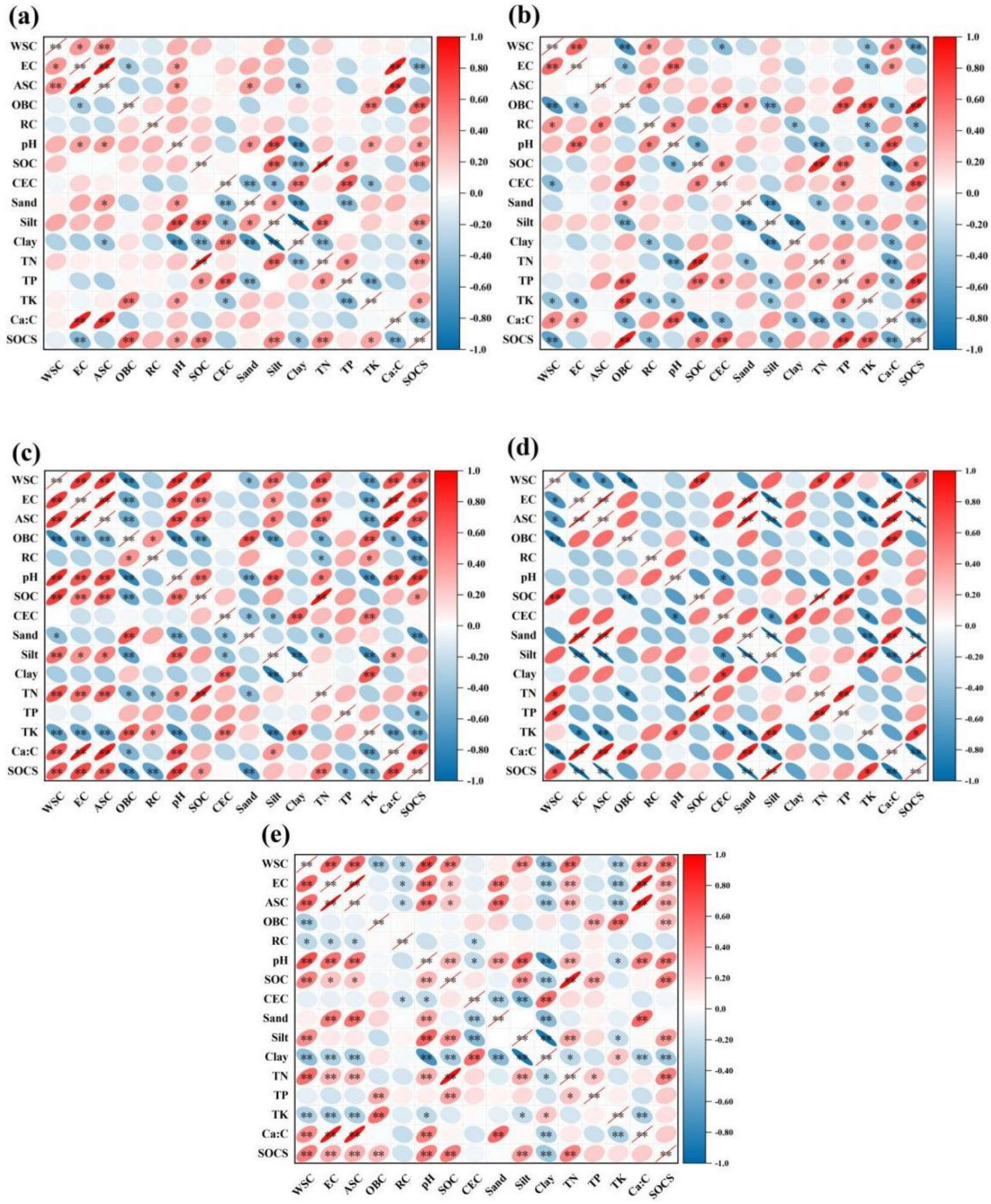

Figure 8. *Correlation analysis of soil calcium carbon under different acidification conditions. NO: strong acidification; (b) weak neutral acidification; (c) neutral; (d) alkaline; (e) No differentiation of acidification gradients; *p < 0.05; **p < 0.01*

Under strongly acidic soil conditions (pH < 4.5), the statistical analysis identified significant correlations among the key parameters ($p < 0.05$). Trivariate association analysis revealed that SOC concentration, SOCS, and Ca/C ratio exhibited distinct patterns in TP availability and CEC levels. Both SOC and SOCS showed significant positive correlations with TP and CEC ($p < 0.05$), in contrast to the negative correlations observed for the Ca/C ratio ($p < 0.05$). Multivariate analysis indicated that calcium speciation played a regulatory role, with OBC and WSC fractions significantly influencing SOC storage dynamics and calcium-carbon equilibrium ($p < 0.05$).

http://www.aloki.hu ● ISSN 1589 1623 (Print) ● ISSN1785 0037 (Online)
DOI: http://dx.doi.org/10.15666/aeer/2401_885903

Structural equation modeling results demonstrated that soil acidification dynamics in Hunan karst cultivated lands enhanced carbon storage through two primary mechanisms: increased concentrations of TN, TP, TK, and SOC in soil nutrients and elevated levels of WSC, EC, and OBC in calcium forms (*Figure 9*). Concurrently, modifications in textural composition positively influenced carbon stocks by increasing TN, TP, TK, SOC, and the ratio of RC to ASC while decreasing CEC and the concentrations of WSC, EC, and OBC. A comprehensive analysis revealed that changes in acidification and soil texture exert both direct and pathway-mediated effects on carbon storage. The intensity of acidification indirectly influenced carbon storage by positively modulating calcium forms and nutrient profiles, whereas textural characteristics mediated these effects through nutrient enhancement and the suppression of calcium forms. Importantly, acidification-driven transformations in calcium speciation and nutrient dynamics were identified as critical predictors of variability in carbon storage in karst agroecosystems.

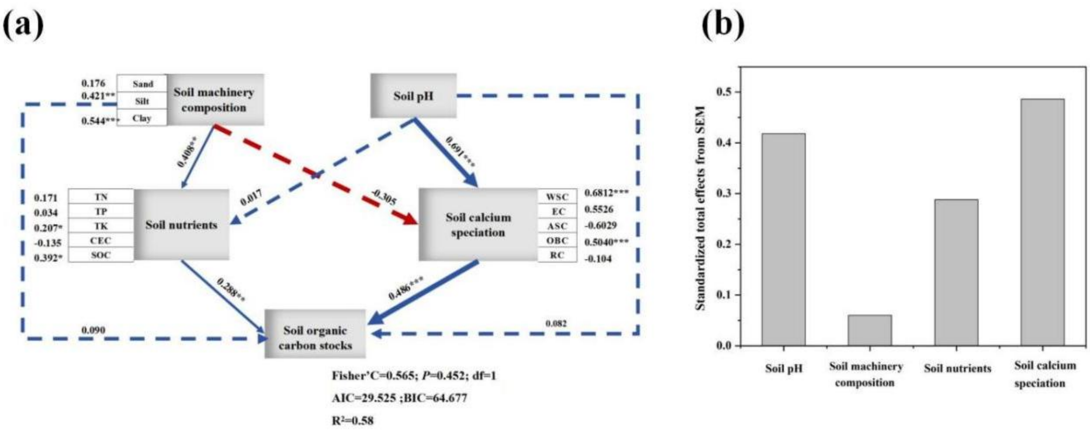

Figure 9. *Modeling karst soil responses: SEM approach to calcium speciation and organic carbon behavior under acidification in Hunan cultivated lands*

Discussion

Calcareous soils, formed by the weathering of carbonate rocks in karst ecosystems, inherently exhibit elevated calcium concentrations under undisturbed natural conditions (Li et al., 2019). Our experimental results demonstrated that acidic environments significantly reduce both calcium and organic carbon content compared with neutral-alkaline conditions. A decline in pH impairs calcium bioavailability, structural stability, and hydrological function. The pH-dependent competitive behavior of Ca^{2+} ions is primarily influenced by several geochemical processes, including the dissolution dynamics of sparingly soluble compounds, hydrolysis of metal-chelate complexes, redox transformations, and surface adsorption-desorption equilibria. Notably, calcium demonstrates superior capacity for ligand competition in neutral-to-alkaline soils ($pH \geq 7$), where pH predominantly regulates its speciation (Yang et al., 2017). The observed accumulation of SOC in alkaline calcareous soils aligns with the well-documented carbonate-enhanced stabilization mechanisms (Fernández-Ugalde et al., 2011). The sequential distribution of the calcium fractions across the acidification gradients was as follows: EC > ASC > WSC > RC > OBC. Progressive acidification leads to substantial reductions in WSC, EC, and ASC pools. EC showed a significant positive correlation with soil pH ($p < 0.05$), underscoring the critical role of pH in controlling

http://www.aloki.hu ● ISSN 1589 1623 (Print) ● ISSN1785 0037 (Online)
DOI: http://dx.doi.org/10.15666/aeer/2401_885903

calcium speciation. This pH-dependent biogeochemical behavior highlights the vulnerability of karst agricultural systems to acidification-induced calcium depletion and its subsequent ecological impacts. Yang et al. (2017) established through initial investigations in Guilin's Yaji karst region that soil pH demonstrates positive correlations with reducible calcium, ASC, and RC fractions while exhibiting a negative correlation with oxidizable calcium. This relationship was subsequently confirmed by Huang et al. (2015) who observed significant pH-calcium correlations across diverse land-use patterns in karst areas. This was further validated through comprehensive analyses of the fault basin ecosystems conducted by Li et al. (2019). The predominance of EC in limestone-derived agricultural soils results from an inherent abundance of carbonates and prolonged agricultural practices. In contrast to the limited organo-calcium complexes associated with residual fractions, this bioavailable calcium exhibits high geochemical mobility and biological accessibility (Huang et al., 2023). These phenomena likely arise from simplified ecosystem structures, low humus content, and intensive leaching processes, which are characteristic of karst environments. Comprehensive studies have shown that in addition to pH, essential soil attributes such as organic carbon content, CEC, and particle size distribution (sand, silt, and clay) significantly influence calcium distribution patterns in terrestrial ecosystems (Cardoso et al., 2020; Razzaghi et al., 2021). Comparative analyses revealed stronger associations between organic matter and both acid-soluble and complexed calcium forms in acidic environments than in neutral-alkaline environments (Robert et al., 2004). Calcium enrichment enhances the synthesis of humic acids in soil organic matrices, facilitating the formation of insoluble metallic ions (Ca-Fe-Mg), which improves ionic nutrient retention and carbon stabilization (Wang et al., 2018). This connection illustrates a bidirectional regulatory relationship with organic carbon levels that simultaneously influences calcium dynamics through intricate biogeochemical feedback mechanisms. In karst ecosystems, soil colloids preferentially adsorb Ca^{2+} and Mg^{2+}. Acidic conditions facilitate the release of ASC into active forms that transition to exchangeable states, thereby enhancing the adsorption capacity of colloidal Ca^{2+} (Li et al., 2019). This mechanism is supported by our observation of a positive correlation between the CEC and ASC under low pH conditions. Notably, clay content exhibited an inverse relationship with all forms of calcium in acidic soils, a phenomenon that may be attributed to the intensive leaching processes characteristic of the subtropical monsoon climate in Hunan. The region's high levels of precipitation and temperature promote soil acidification through the depletion of base cations, resulting in colloidal surfaces dominated by acid-forming ions, rather than nutrient cations.

Global research indicates a positive correlation between EC in clay minerals and SOC levels in slightly acidic to alkaline soils (Rasmussen et al., 2018; Rowley et al., 2021). This mechanistic understanding is supported by field data from Hunan's karst agricultural regions, where increasing soil acidification has led to significant declines in organic carbon content, storage capacity, and Ca/C ratios, reaching minimal levels under severe acidification. Statistical analysis revealed a significant association ($p < 0.05$) between total calcium levels and variations in SOC. Calcium facilitates physicochemical interactions at organic-mineral interfaces through processes, such as adsorption, coprecipitation, complexation, and aggregation occlusion. These mechanisms reduce the bioavailability of SOC while enhancing its persistence and SOCS (Shabtai et al., 2023). Understanding the dynamics of calcium pools during acidification is crucial for managing organic carbon reservoirs and improving the soil quality in Hunan's karst agricultural systems.

http://www.aloki.hu ● ISSN 1589 1623 (Print) ● ISSN1785 0037 (Online)
DOI: http://dx.doi.org/10.15666/aeer/2401_885903

Conclusion

The karst-cultivated soils in Hunan Province exhibited an average SOC concentration of 13.08 g kg^{-1}, with statistically significant differences in SOC storage ($p < 0.05$). Both SOC measures peaked under neutral conditions and showed a gradual decline as acidity increased. In highly acidic environments, calcium and carbon metrics reached their lowest levels, with reductions of 34.3–44.4% in SOC content and 28.4–41.4% in storage compared with neutral-alkaline conditions. The results of the calcium speciation analysis revealed that the exchangeable form predominated at 13.4 g kg^{-1}, indicating considerable mobility. The forms were arranged in the following order: EC > ASC > WSC > RC > OBC. Notably, the competitiveness of Ca^{2+} decreased by a factor of 215, along the acidification gradient. Soil acidification was the primary factor influencing calcium conversion and nutrient dynamics and served as a crucial predictor of carbon storage. Enhancing strategic SOC management is essential for activating the acid-buffering potential of Ca^{2+} in karst agroecosystems.

Acknowledgements. This research was funded by the Open Fund of Guangxi Key Laboratory of Karst Dynamics, Ministry of Natural Resources, China (KDL & Guangxi 202010), the National Key R&D Program, Ministry of Science and Technology of China (2022YFD1700103-306), and Key Projects of Hunan Provincial Department of Education (23A0185).

REFERENCES

[1] Cao, J. H., Yuan, D. X., Zhang, C. (2004): Karst ecosystem constrained by geological conditions in Southwest China. – Earth and Environment 32(01): 1-8.

[2] Cardoso, R., Pedreira, R., Duarte, S. O. D., Monteiro, G. A. (2020): About calcium carbonate precipitation on sand biocementation. – Engineering Geology 271: 105612. https://doi.org/10.1016/j.enggeo.2020.105612.

[3] Dion, K., Bodnaruc, A. M., Trudel, G., Lamarche, J., Ranger, V., Fobert, S., Church, K. A., Mukunzi, J. N., Rene, J. L. (2021): Structural equation modeling - an accompanying guide for the R interface. – Quantitative Methods for Psychology 17(3): 198-271.

[4] Dong, L. G. (2019): A method for determining soil physical properties by undisturbed soil sample. – Journal of Ningxia Agriculture and Forestry Science and Technology 60(04): 51-52.

[5] Duan, L., Chen, X., Ma, X., Zhao, B., Thorjorn, L., Wang, S., Ye, Z. (2016): Atmospheric S and N deposition relates to increasing riverine transport of S and N in southwest China: Implications for soil acidification. – Environmental Pollution 218: 1191-1199. https://doi.org/10.1016/j.envpol.2016.08.075.

[6] Fan, J. Q., Wang, L., Qin, J. X., Zhang, F. R., Xu, Y. (2020): Evaluating cultivated land stability during the growing season based on precipitation in the Horqin Sandy Land, China. – Journal of Environmental Management 276: 111269. https://doi.org/10.1016/j.jenvman.2020.111269.

[7] Fernández-Ugalde, O., Virto, I., Barré, P., Gartzia-Bengoetxea, N., Enrique, A., Imaz, M. J., Bescansa, P. (2011): Effect of carbonates on the hierarchical model of aggregation in calcareous semi-arid Mediterranean soils. – Geoderma 164(3-4): 203-214. https://doi.org/10.1016/j.geoderma.2011.06.008.

[8] Gao, L., Wang, W., Liao, X., Tan, X., Yue, J., Zhang, W., Wu, J., Willison, J. H. M., Tian, Q., Liu, Y. (2023): Soil nutrients, enzyme activities, and bacterial communities in varied plant communities in karst rocky desertification regions in Wushan County, Southwest China. – Frontiers in Microbiology 14: 1180562.

https://doi.org/10.3389/fmicb.2023.1180562.
[9] Gu, F., Yung, Y. F., Cheung, M. W. L., Joo, B. K., Nimon, K. (2023): Statistical inference in redundancy analysis: a direct covariance structure modeling approach. – Multivariate Behavioral Research 58(5): 877-893. DOI:10.1080/00273171.2022.2141675.
[10] Hen, R. L., Hao, Y. L., Jiang, S. F. (2014): Present situation and repair methods of soil heavy metal pollution. – Western Resources 6: 137-139.
[11] Huang, F., Hu, G., Tu, Y. C., Fan, M. Z., Cao, J. H. (2015): Fraction distribution of calcium in soils of different land use types in Karst areas. – Journal of Southern Agriculture 46(09): 1574-1578.
[12] Huang, M. Z., Lan, J. C., Wang, S. S., Wang, J. X., Qi, X., Liu, L., Yue, K. Q. (2024): Effects of soil exchangeable calcium in promoting the accumulation of soil organic carbon by Karst vegetation restoration. – Journal of Soil Science and Plant Nutrition 24(2): 843-854. https://doi.org/10.1007/s42729-023-01589-6.
[13] Jiang, X. S., Guo, Y., Li, H. X., Li, X. M., Liu, J. (2022): Ecological evolution during the three-year restoration using rhizosphere soil cover method at a Lead-Zinc tailing pond in Karst areas. – Science of the Total Environment 853: 158291. https://doi.org/10.1016/j.scitotenv.2022.158291.
[14] Li, W., Yu, L. J., He, Q. F., Wu, Y., Yuan, D. X., Cao, J. H. (2004): Effects of microbes and their carbonic anhydrase on Ca^{2+} and Mg^{2+} migration in column-built leached soil-limestone karst systems. – Applied Soil Ecology 29(3): 274-281. DOI:10.1016/j.apsoil.2004.12.001.
[15] Li, S. X., Wang, D. Y. (2005): A study of the acidification of purple soil in Chongqing in recent two decades. – Journal of Chongqing Normal University (Natural Science) 22(1): 70-73.
[16] Li, G. C. (2012): The migration of calcium in the soil and its effect of ecological under *Castanea mollissima* trees in typical karst area. – Dissertation, Guangxi Normal University.
[17] Li, H. L., Gong, L., Zhu, M. L., Liu, Z. Y., Xie, L. N., Hong, Y. (2015): Stoichiometric characteristics of soil in an oasis on northern edge of Tarim Basin, China. – Acta Pedologica Sinica 52(06): 1345-1355.
[18] Li, Z. Y., Wei, X. H., Li, B. S., Guan, G. C., Xu, X. Z., Lei, L. (2016): Spatial distribution of soil calcium on natural slope of karst peak-cluster in northern Guangdong Province. – Bulletin of Soil and Water Conservation 36(3): 62-68.
[19] Li, Q., Yang, C., Jin, Z. J., Zhu, T. B., Cao, J. H. (2019): Characteristics of calcium fraction distribution in soil under different land use types in Karst fault-depression basins. – Carsologica Sinica 38(6): 889-895. DOI: 10.11932/karst2019y14.
[20] Lin, H. L. (2022): Mechanism and application of magnesium fertilizer in improving soil acidification in tea garden. – Dissertation, Fujian Agriculture and Forestry University.
[21] Liu, C. N., Huang, Y., Wu, F., Liu, W. J., Ning, Y. Q., Huang, Z. R., Tang, S. Q., Liang, Y. (2021): Plant adaptability in karst regions. – Journal of Plant Research 134(5): 889-906. https://doi.org/10.1007/s10265-021-01330-3.
[22] Luo, Y. M., Teng, Y. (2018): Regional difference in soil pollution and strategy of soil zonal governance and remediation in China. – Bulletin of Chinese Academy of Sciences 33(2): 145-152. DOI: https://doi.org/10.16418/j.issn.1000-3045.2018.02.003.
[23] Ma, T. S., Deng, X. W., Chen, L., Xiang, W. H. (2020): The soil properties and their effects on plant diversity in different degrees of rocky desertification. – Science of the Total Environment 736: 139667. https://doi.org/10.1016/j.scitotenv.2020.139667.
[24] Nava, A. R., Mauricio, N., Sanca, A. J., Domínguez, D. C. (2020): Evidence of calcium signaling and modulation of the LmrS multidrug resistant efflux pump activity by Ca^{2+} ions in *S. aureus*. – Frontiers in Microbiology 11: 2463. https://doi.org/10.3389/fmicb.2020.573388.
[25] Qiu, G. J., Xing, X. N., Cong, G. Q., Yang, X. Y. (2023): Measuring the cultivated land use efficiency in China: a super efficiency MinDS model approach. – International Journal of Environmental Research and Public Health 20(1): 583.

https://doi.org/10.3390/ijerph20010583.
[26] Rasmussen, C., Heckman, K., Wieder, W. R., Keiluweit, M., Wagai, R. (2018): Beyond clay: towards an improved set of variables for predicting soil organic matter content. – Biogeochemistry 137: 297-306. https://doi.org/10.1007/s10533-018-0424-3.
[27] Razzaghi, F., Arthur, E., Moosavi, A. A. (2021): Evaluating models to estimate cation exchange capacity of calcareous soils. – Geoderma 400: 115225. https://doi.org/10.1016/j.geoderma.2021.115221.
[28] Rowley, M. C., Grand, S., Spangenberg, J. E., Verrecchia, E. P. (2021): Evidence linking calcium to increased organo-mineral association in soils. – Biogeochemistry 153(3): 223-241. https://doi.org/10.1007/s10533-021-00779-7.
[29] Sanchez-Rodriguez, M. I., Sanchez-Lopez, E., Marinas, A., Caridad, J. M., Urbano, F. J. (2022): Redundancy analysis to reduce the high-dimensional near-infrared spectral information to improve the authentication of olive oil. – Journal of Chemical Information and Modeling 62(19): 4620-4628. https://doi.org/10.1021/acs.jcim.2c00964.
[30] Shabtai, I. A., Wilhelm, R. C., Schweizer, S. A., Höschen, C., Buckley, D. H., Lehmann, J. (2023): Calcium promotes persistent soil organic matter by altering microbial transformation of plant litter. – Nat Commun 14: 6609. https://doi.org/10.1038/s41467-023-42291-6.
[31] Tao, L., Li, F. B., Liu, C. S., Feng, X. H., Gu, L. L., Wang, B. R., Wen, S. L., Xu, M. G. (2019): Mitigation of soil acidification through changes in soil mineralogy due to long-term fertilization in southern China. – Catena 174: 227-234. https://doi.org/10.1016/j.catena.2018.11.023.
[32] Wang, L. J., Wang, P., Sheng, M. Y. (2018): Stoichiometric characteristics of soil nutrient elements and its influencing factors in typical Karst rocky desertification ecosystems, Southwest China. – Acta Ecologica Sinica 38(18): 6580-6593. DOI:10.5846/stxb201803290635.
[33] Wei, X. H., Lei, L., Liu, S. J., Guan, G. C. (2017): Analysis on the absorbing, transfer, restoration and adaptation mechanism of calcium in different peak forest plants in northern Guangdong Province, China. – Carsologica Sinica 36(3): 368-376. DOI:10.11932/karst20170311.
[34] Wen, X., Li, M. D., Tu, X. D., Wu, H. Y., Xia, H. A., Liu, Q. F. (2013): Acidification problems of arable land in Hunan Province and its improvement countermeasures. – Hunan Agricultural Sciences 2013(10): 56-60.
[35] Wu, Y. J., Tian, X., Wang, R. Z., Zhang, M. Y., Wang, S. (2023): Effects of vegetation restoration on distribution characteristics of heavy metals in soil in Karst plateau area of Guizhou. – PeerJ 11: e15044. DOI:10.7717/peerj.15044.
[36] Xiao, S. Y., Shu, Y. G., Chen, M. J. (2019): Soil anti-erodibility under different vegetation types in Karst Plateau Gorge Region. – Bulletin of Soil and Water Conservation 39(4): 30-35, 81. https://doi.org/10.13961/j.cnki.stbctb.20190703.001.
[37] Xu, R. K., Li, J. Y., Zhou, S. W., Xu, M. G., Sheng, R. F. (2018): Scientific issues and controlling strategies of soil acidification of croplands in China. – Bulletin of Chinese Academy of Sciences 33(2): 160-167. https://doi.org/10.16418/j.issn.1000-3045.2018.02.005.
[38] Yang, H., Liang, J. H., Chen, J. R., Cao, J. H. (2015): Soil calcium speciation at different geomorphological positions in the Yaji Karst Experimental Site in Guilin, China. – Journal of Resources and Ecology 6(4): 224-229. https://doi.org/10.5814/j.issn.1674-764X.2015.04.005.
[39] Yang, H., Chen, J. R., Liang, J. H., Cao, J. H. (2017): Preliminary study on the relationship between soil organic carbon and pH value and calcium species in Yaji Karst Region, Guilin. – Geological Review 63(4): 1117-1126.
[40] Yang, S. T., Li, X., Lou, H. Z., Luo, Y., Li, C. J., Wang, P. F., Wu, X. J., Zhang, J. (2021): Spatial estimation model and migration analysis of soil total calcium content in the Maolan Karst Area, Guizhou Province. – Carsologica Sinica 40(3): 449-458.

[41] Yi, X., Tao, W. L., Zhou, H. H., Zhu, S. W., Wang, X. Y., Dong, Z. L., Gao, S. Y., Li, X. K., Song, X. X. (2025): Parent soil type modulates biochar and mowing effects on soil microbial communities in karst region. – Frontiers in Microbiology 16. https://doi.org/10.3389/fmicb.2025.1680847.
[42] Yu, H., Wang, S. J. (2007): A new sequential extraction of calcium species in soil samples. – Rock and Mineral Analysis 2007(6): 436-440.
[43] Zhang, Y. H., Xu, X. L., Li, Z. W., Xu, C. H., Luo, W. (2021): Improvements in soil quality with vegetation succession in subtropical China karst. – Science of the Total Environment 775: 145876. https://doi.org/10.1016/j.scitotenv.2021.145876.
[44] Zhang, D. D., Zheng, X. Q., Li, H. Y., Chen, P. Z., Kong, H., Huang, Z. P. (2022): Effects of rural domestic irrigation with different salinity on soil microorganisms. – Research of Environmental Sciences 35(8): 1873-1884. DOI:10.13198/j.issn.1001-6929.2022.05.01.
[45] Zhang, W. Q., Qie, R. Q. (2024): Spatiotemporal change of cultivated land in China during 2000-2020. – PLoS ONE 19(1): e0293082. https://doi.org/10.1371/journal.pone.0293082.
[46] Zhou, S. J., Zhao, S. K., Jiang, H., Li, J. (2020): Distribution pattern and characteristics of rocky desertification land in Karst areas of Hunan Province. – Journal of Green Science and Technology 14: 56-57.

APPENDIX

***Table A1.** Details of sampling points and related information*

Soil profile	Sampling Location	Elevations	Latitude	Longitude	Land use patterns	Vegetation coverage
ZJJ02	Cili	284 m	110.9 E	29.3 N	Farmland to shrubland conversion	40–80%
ZJJ03	Yongding	510 m	110.4 E	29.0 N	Paddy-to-dryland conversion	40%
XX04	Longshan	123 m	109.3 E	28.8 N	Farmland to grassland conversion	≥80%
XX05	Baojing	365 m	109.4 E	28.8 N	Farmland to shrubland conversion	≥80%
XX09	Jishou	606 m	109.5 E	28.3 N	Paddy field	≥80%
XX12	Longshan	550 m	109.4 E	29.3 N	Paddy field	≥80%
CZ04	Linwu	404 m	112.5 E	25.5 N	Farmland to shrubland conversion	≥70%
CZ05	Jiahe	255 m	112.5 E	25.6 N	Farmland to shrubland conversion	60%
CZ11	Guiyang	205 m	112.7 E	25.8 N	Paddy field	≥80%
SY04	Chengbu	462 m	110.3 E	26.4 N	Farmland to shrubland conversion	≥80%
SY11	Shaodong	254 m	111.7 E	27.2 N	Paddy field	40–80%
SY13	Shanyang	259 m	111.2 E	26.8 N	Paddy field	≥80%
YZ08	Xintian	380 m	112.1 E	25.8 N	Forest land	≥70%
YZ10	Qiyang	117 m	111.8 E	26.7 N	Paddy field	≥80%
YZ11	Lingling	131 m	111.5 E	26.1 N	Paddy field	≥80%
LD01	Lianyuan	174 m	111.7 E	27.7 N	Farmland to forest conversion	40–80%
LD05	Louxing	146 m	111.9 E	27.7 N	Paddy field	40–80%
LD02	Xintian	440 m	111.5 E	27.9 N	Farmland to forest conversion	40–80%
ZZ05	Yanling	263 m	113.7 E	26.4 N	Farmland to shrubland conversion	30%
HY02	Changning	92 m	112.6 E	26.4 N	Farmland to forest conversion	40–80%

http://www.aloki.hu ● ISSN 1589 1623 (Print) ● ISSN1785 0037 (Online)
DOI: http://dx.doi.org/10.15666/aeer/2401_885903

***Table A2.** Methods of calcium speciation extraction*

Speciation of calcium in soil	Extractant	Operating procedure
WSC	Distilled water	Oscillation at 200 times/min for 2 hours, centrifugation at 3000 rpm for 30 min, and determination using AAS method
EC	1 mol/L $AlCl_3$ solution	Oscillation at 200 times/min for 2 hours, centrifugation at 3000 rpm for 30 min, and determination using AAS method
ASC	3 mol/L HCl solution	Shaking in a constant temperature water bath at 80°C for 2 hours, centrifugation at 3000 rpm for 30 min, and determination using AAS method
OBC	0.5 mol/L Na_2SO_4 solution	Shaking at 200 times/min for 2 hours, standing for 24 hours, centrifugation at 3000 rpm for 30 min, and determination using AAS method
RC	HNO_3 + HF solution	Drying, regrinding, digestion with HNO_3 and HF, and determination using AAS method

http://www.aloki.hu ● ISSN 1589 1623 (Print) ● ISSN1785 0037 (Online)
DOI: http://dx.doi.org/10.15666/aeer/2401_885903